

Charge-Dependence of the Nucleon-Nucleon Interaction

G. Q. Li* and R. Machleidt†

Department of Physics, University of Idaho, Moscow, ID 83844, U.S.A.

(June 21, 2021)

Based upon the Bonn meson-exchange-model for the nucleon-nucleon (NN) interaction, we calculate the charge-independence breaking (CIB) of the NN interaction due to pion-mass splitting. Besides the one-pion-exchange (OPE), we take into account the 2π -exchange model and contributions from three and four irreducible pion exchanges. We calculate the CIB differences in the 1S_0 effective range parameters as well as phase shift differences for partial waves up to total angular momentum $J = 4$ and laboratory energies below 300 MeV. We find that the CIB effect from OPE dominates in all partial waves. However, the CIB effects from the 2π model are noticeable up to D-waves and amount to about 40% of the OPE CIB-contribution in some partial waves, at 300 MeV. The effects from 3π and 4π contributions are negligible except in 1S_0 and 3P_2 .

*Present Address: Department of Physics, SUNY, Stony Brook, NY 11794

†Electronic address: machleid@uidaho.edu

I. INTRODUCTION

It is well known that isospin invariance is not an exact symmetry of strong interactions. Consequently, nuclear forces have a small but measurable charge-dependent component. The equality between proton-proton (pp) [or neutron-neutron (nn)] and neutron-proton (np) nuclear interactions is known as charge independence. Charge-independence breaking (CIB) is seen most clearly in the 1S_0 nucleon-nucleon (NN) scattering lengths. The latest empirical values for the singlet scattering length a and effective range r are [1]:

$$\begin{aligned} a_{pp}^N &= -17.3 \pm 0.4 \text{ fm}, & r_{pp}^N &= 2.85 \pm 0.04 \text{ fm}, \\ a_{nn}^N &= -18.8 \pm 0.3 \text{ fm}, & r_{nn}^N &= 2.75 \pm 0.11 \text{ fm}, \\ a_{np} &= -23.75 \pm 0.01 \text{ fm}, & r_{np} &= 2.75 \pm 0.05 \text{ fm}. \end{aligned} \quad (1)$$

The values given for pp and nn scattering refer to the nuclear part of the interaction as indicated by the superscript N . Electromagnetic effects have been removed from the experimental values, which is model dependent. The uncertainties quoted for a_{pp}^N and r_{pp}^N are mainly due to this model dependence.

It is useful to define the following averages:

$$\bar{a} \equiv \frac{1}{2}(a_{pp}^N + a_{nn}^N) = -18.05 \pm 0.5 \text{ fm}, \quad (2)$$

$$\bar{r} \equiv \frac{1}{2}(r_{pp}^N + r_{nn}^N) = 2.80 \pm 0.12 \text{ fm}. \quad (3)$$

By definition, CIB is the difference between the np values and these averages:

$$\Delta a_{CIB} \equiv \bar{a} - a_{np} = 5.7 \pm 0.5 \text{ fm}, \quad (4)$$

$$\Delta r_{CIB} \equiv \bar{r} - r_{np} = 0.05 \pm 0.13 \text{ fm}. \quad (5)$$

Thus, the NN singlet scattering length shows a clear signature of CIB in strong interactions.

Charge dependence of NN interactions has been the subject of extensive investigations, both experimentally and theoretically, for many decades (for recent reviews, see Refs. [1,2]). The current understanding is that the charge dependence of nuclear forces is due to differences in the up and down quark masses and electromagnetic interactions. On a more phenomenological level, major causes of CIB are:

- mass splitting of isovector mesons; particularly, π and ρ ;
- irreducible pion-photon exchanges.

It has been known for a long time that the difference between the charged and neutral pion masses in the one-pion-exchange (OPE) potential accounts for about 50% of Δa_{CIB} . In Ref. [3], charge dependent interactions were derived for np and pp scattering, based on a preliminary version of the Bonn meson-exchange model [4] taking into

account the pion mass difference in OPE as well as two-boson exchanges. With these interactions, about 80% of the empirical Δa_{CIB} could be explained. Earlier, Ericson and Miller [5] had obtained a very similar result using the meson-exchange model of Partovi and Lomon [6].

The calculations of Refs. [3,5] were performed only for the singlet scattering length. However, it is also of interest to know the charge-dependent effects for intermediate energies and in partial waves other than 1S_0 . Therefore, it is the main purpose of the present investigation to calculate phase shift differences between pp (or nn) and np scattering for states with total angular momentum $J \leq 4$ and laboratory incident kinetic energies $T_{lab} \leq 300$ MeV. This paper complements an earlier one on charge-asymmetry of the NN interaction [7].

In Sect. II, we will discuss various classes of irreducible meson-exchange diagrams and calculate their CIB effects—due to pion-mass splitting—on NN phase shifts and singlet effective range parameters. Summary and conclusions are given in Sect. III.

II. THE BONN MODEL AND CHARGE-DEPENDENCE

The Bonn meson-exchange model for the NN interaction has been described in detail in the literature [8–10]. It is a field-theoretic model that, apart from the well-known one-boson-exchange terms, includes an explicit model for the 2π -exchange, $\pi\rho$ diagrams, and some further contributions of 3π - and 4π -exchange. The Bonn model yields an excellent description of the NN scattering data below pion production threshold [10] and, thus, provides a reliable basis for an investigation of the charge dependence of the NN interaction. Within the model, charge-dependence is created by the mass difference between the charge-states of mesons. The Bonn model includes three isovector mesons, namely, π , $\rho(770)$, and $a_0/\delta(980)$. We will focus here mainly on the charge-dependent effects due to pion mass difference. Effects due to rho-mass splitting will be discussed briefly at the end of this section, and mass splitting of the $a_0/\delta(980)$ will be ignored since nothing is known.

We use averages for the baryon masses: the average nucleon mass $M_N = 938.919$ MeV and the average Δ -mass $M_\Delta = 1232$ MeV. The pion masses are

$$m_{\pi^\pm} = 139.568 \text{ MeV}, \quad m_{\pi^0} = 134.974 \text{ MeV}. \quad (6)$$

The values are based upon the 1992 Review of Particle Properties [11].

The interaction Lagrangians involving pions are

$$\mathcal{L}_{\pi NN} = \frac{f_{\pi NN}}{m_{\pi^\pm}} \bar{\psi} \gamma_\mu \gamma_5 \tau \psi \cdot \partial^\mu \varphi_\pi, \quad (7)$$

$$\mathcal{L}_{\pi N\Delta} = \frac{f_{\pi N\Delta}}{m_{\pi^\pm}} \bar{\psi} T \psi_\mu \cdot \partial^\mu \varphi_\pi + \text{H.c.}, \quad (8)$$

with ψ the nucleon, ψ_μ the Δ (Rarita-Schwinger spinor), and φ_π the pion fields. τ are the usual Pauli matrices describing isospin 1/2 and \mathbf{T} is the isospin transition operator. $H.c.$ denotes the Hermitean conjugate.

The Lagrangians are divided by m_{π^\pm} to make the coupling constants f dimensionless. Following established conventions [12], we always use m_{π^\pm} as scaling mass. It may be tempting to use m_{π^0} for π^0 coupling. Notice, however, that the scaling mass could be anything. Therefore, it is reasonable to keep the scaling mass constant within SU(3) multiplets [12]. This avoids the creation of unmotivated CIB.

In our investigation of charge-dependent effects on the NN interaction, we start from a case that may be denoted the average between pp and nn scattering. For this case, our model yields -18.05 fm for the singlet scattering length and 2.864 fm for the effective range, consistent with Eqs. (2) and (3). The one-pion-exchange contribution for this average case is depicted in Fig. 1a and 2π -exchange contributions are shown in Fig. 2a, 3a, and 4a. Note that, in this case, the proton ‘p’ in Figs. 1a to 4a carries the average nucleon mass of 938.919 MeV and there are no electromagnetic interactions; equally well, one may use a neutron ‘n’ in place of the proton in part (a) of all figures.

To calculate the effects of charge dependence on the NN phase shifts, we introduce for each LSJ state the CIB phase shift difference $\Delta\delta_{CIB}^{LSJ}(T_{lab})$, defined by

$$\Delta\delta_{CIB}^{LSJ}(T_{lab}) \equiv \delta_{np}^{LSJ}(T_{lab}) - \bar{\delta}^{LSJ}(T_{lab}) \quad (9)$$

where $\bar{\delta}^{LSJ}$ denotes the average of the pp and nn phase shifts which, as discussed, is calculated by taking the diagrams Figs. 1a to 4a into account (besides the other diagrams involved in the Bonn model) with average nucleon mass and all electromagnetic interactions switched off. The phase shift δ_{np}^{LSJ} is the np one to be calculated below. Similarly, we define the CIB mixing parameter difference $\Delta\epsilon_{CIB}^J$,

$$\Delta\epsilon_{CIB}^J(T_{lab}) \equiv \epsilon_{np}^J(T_{lab}) - \bar{\epsilon}^J(T_{lab}). \quad (10)$$

The charge-dependence generated by the model under consideration is now ‘switched on’ step by step:

1. **One-pion-exchange (OPE), Fig. 1:** The CIB effect is created by replacing the diagram of Fig. 1a by the two diagrams of Fig. 1b. Note that one-meson-exchange contributions are roughly proportional to $1/m_\alpha^2$ (with m_α the meson mass) because this is approximately the momentum-space one-meson propagator for very low momentum transfer. Thus, since the π^0 has a smaller mass than the π^\pm , π^0 exchange is stronger than π^\pm exchange. For this reason, OPE is stronger in pp as compared to np . Since OPE is repulsive in 1S_0 , this phase shift becomes more attractive (i. e., larger) when going from pp to np , resulting in a positive $\Delta\delta$;

cf. column ‘OPE’ in Table I and dashed curve in Fig. 5. Consistent with this is the well-known fact that OPE takes care of about 50% of Δa_{CIB} . In the other partial waves, the sign of $\Delta\delta$ due to OPE depends on if OPE is repulsive or attractive (e. g., it is repulsive in 3P_1 and attractive in 3P_0 and 3P_2). Due to the small mass of the pion, OPE is a sizable contribution in all partial waves including higher partial waves; and due to the pion’s relatively large mass splitting (3.4%), OPE creates relatively large charge-dependent effects in all partial waves (Fig. 5 and Table I).

2. **2π -exchange with NN intermediate states ($2\pi NN$), Fig 2:** Notice first that only non-iterative (irreducible) diagrams are to be considered, since the iterative ones are generated by the scattering equation from OPE. We mention here that, in our approach which is based upon time-ordered perturbation theory, we always take all time-orderings into account (except for those that imply antibaryons in intermediate states); however, to save space, we display only a few characteristic time-orderings in Fig. 2 (this is also true for all diagrams shown in Figs. 3 and 4; to get an impression of the total number of time-ordered diagrams, see Fig. 20 of Ref. [8]). The CIB effect is obtained by replacing the diagrams Fig. 2a (pp/nn scattering) by those of Fig. 2b (np scattering). For a good understanding of CIB effects, it is important to distinguish between box (here: stretched box) and crossed box diagrams. Concerning the effect from stretched box diagrams, one replaces the left diagram of Fig. 2a by the four stretched box diagrams of Fig. 2b (and similarly for the other stretched box time-orderings not shown). Notice now that in the former diagram two π^0 are exchanged making this a ‘strong’ diagram, while the latter four diagrams together with their isospin factors result in a weaker contribution. Since 2π exchange is, in general, attractive, there is a loss of attraction when going from pp to np (equivalent to a reduction of the phase shift). This qualitative estimate is clearly confirmed by the quantitative results displayed in column ‘ $2\pi NN - S$ ’ of Table II. The CIB effect that stems from crossed box diagrams is obtained by replacing the two crossed boxes of Fig. 2a by the three crossed boxes of Fig. 2b. Typically, this effect (column ‘ $2\pi NN - X$ ’ of Table II) is of opposite sign as compared to the corresponding (stretched) box effect, in most partial waves. The total CIB effect from all diagrams of Fig. 2 is displayed by the dashed curve in Fig. 6.

3. **2π -exchange with $N\Delta$ intermediate states ($2\pi N\Delta$), Fig. 3:** Notice again, that every box stands for all possible time-orderings of the box type (diagrams 1 to 6 of Fig. 20 of Ref. [8]) and

every crossed box for all possible time-orderings of the crossed box type (diagrams 7 to 12 of Fig. 20 of Ref. [8]). Thus, the total number of diagrams which Fig. 3a stands for is 24 while Fig. 3b stands for 48 diagrams, which are all explicitly taken into account in our calculations. Replacement of the boxes Fig. 3a by the boxes Fig. 3b causes an increase in the strength of these diagrams which, since these are attractive diagrams, causes an increase in attraction. Column ‘ $2\pi N\Delta - B$ ’ in Table II clearly confirms this. For the crossed boxes one gets typically the opposite effect (column ‘ $2\pi N\Delta - X$ ’ of Table II). This partial cancelation of the effects from the two groups of diagrams is also demonstrated in Fig. 6 where the dash-dot curve represents the effect from the box diagrams while the dash-triple-dot curve is from the crossed ones. Notice that the cancelation is almost perfect in 1S_0 and 3P_2 even though the individual contributions are rather large.

4. **2π -exchange with $\Delta\Delta$ intermediate states ($2\pi\Delta\Delta$), Fig. 4:** The replacement of the diagrams of Fig. 4a by Fig. 4b shows the by now familiar characteristic: opposite effects from box and crossed box diagrams (column ‘ $2\pi\Delta\Delta - B$ ’ and ‘ $2\pi\Delta\Delta - X$ ’ of Table II). This results in large cancelations between effects which, due to the short-range nature of this class of diagrams, are individually already rather small. This explains why the CIB effect from the diagrams of Fig. 4 is negligible in most partial waves (dotted curve in Fig. 6).

This finishes the discussion of all contributions of the 2π type. In summary, one can say that the total CIB effect from 2π (dash-dot curve in Fig. 5) is quite noticeable up to the D -state. In 1S_0 , 3P_0 , 3P_1 , and 1D_2 , the CIB effect from 2π is 20-50% of the one from OPE, at 300 MeV. However, for low energies (except in 1S_0) as well as in higher partial waves, the CIB 2π effect is negligible.

5. **$\pi\rho$ -exchanges.** This group is, in principal, as comprehensive as the 2π -exchanges discussed above. Graphically, the $\pi\rho$ diagrams can be obtained by replacing in each diagram of Figs. 2–4, one of the two pions by a ρ -meson of the same charge-state (because of this simple analogy, we do not show the $\pi\rho$ diagrams explicitly here). Concerning the $\pi\rho$ diagrams with Δ intermediate states a comment is in place. In the Bonn model [8], the crossed $\pi\rho$ diagrams with $N\Delta$ and $\Delta\Delta$ intermediate states are included in terms of an approximation. It is assumed that they differ from the corresponding box diagrams only by the isospin factor. Thus, the $\pi\rho$ box diagrams with $N\Delta$ and $\Delta\Delta$ intermediate states are multiplied by an isospin factor that is equal to the sum of the isospin factors for box and crossed box. In this approximation, these diagrams do not

generate any CIB effects due to pion-mass splitting. Since these diagrams are of very short range, their CIB effect may be negligible, anyhow. The only class of $\pi\rho$ diagrams which we include in our calculation of CIB effects is the one that corresponds to Fig. 2, with one pion in each diagram replaced by a ρ meson. Its contribution to CIB (column ‘ $\pi\rho$ ’ of Table I and dash-triple-dot curve of Fig. 5) is generally small, and typically opposite to the one from 2π , in most states.

6. **Further 3π and 4π contributions ($\pi\sigma + \pi\omega$).** The Bonn potential also includes some 3π -exchanges that can be approximated in terms of $\pi\sigma$ diagrams and 4π -exchanges of $\pi\omega$ type. It was found in Ref. [8] that the sum of these contributions is small. These diagrams have NN intermediate states—similar to Fig. 2, but with one of the two exchanged pions replaced by an isospin-zero boson; thus, the isospin factors are different from the ones of Fig. 2 and, in fact, like the ones of Fig. 1. Another way of creating these diagrams is to combine the diagrams of Fig. 1 with a sigma or an omega in an irreducible way, i. e., by forming a stretched box or crossed box diagram. These diagrams carry the same isospin factors as OPE. Since this class of diagrams is part of the Bonn model, we include these diagrams in our CIB consideration. The CIB effect from this class is very small, except in 1S_0 , 3P_1 , and 3P_2 (Column ‘ $\pi\sigma + \pi\omega$ ’ of Table I and dotted curve in Fig. 5). This effect has always the same sign as the effect from OPE, but it is substantially smaller. The reason for the OPE character of this contribution is that $\pi\sigma$ prevails over $\pi\omega$ and, thus, determines the character of this contribution. Since sigma-exchange is negative and since, furthermore, the propagator in between the π and the σ exchange is also negative, the overall sign of the $\pi\sigma$ exchange is the same as OPE. Thus, it is like a weak, short-ranged OPE.

This finishes our detailed presentation of the diagrams and their CIB effects included in our calculation. The sum of all CIB effects on phase shifts is given in the last column of Table I and plotted by the solid curve in Fig. 5. Notice that the difference between the solid curve and the dashed curve (OPE) in Fig. 5 represents the sum of all effects beyond OPE. Thus, it is clearly seen that OPE dominates the CIB effect in all partial waves, even though there are substantial contributions besides OPE in some states, notably 1S_0 , 3P_1 , and 1D_2 .

Finally, in Table III and IV, we also give the CIB contributions to the 1S_0 scattering length and effective range. Note that the relationship between the CIB potential and the corresponding change of the scattering length, Δa_{CIB} , is highly non-linear. As discussed in Refs. [5,3], when the scattering length changes from a_1 to a_2 due to a CIB potential $\Delta V = V_1 - V_2$, the relationship is

$$\frac{1}{a_2} - \frac{1}{a_1} = M_N \int_0^\infty \Delta V u_1 u_2 dr \quad (11)$$

or

$$a_1 - a_2 = a_1 a_2 M_N \int_0^\infty \Delta V u_1 u_2 dr, \quad (12)$$

with u_1 and u_2 the zero-energy 1S_0 wave functions normalized such that $u(r \rightarrow \infty) \rightarrow (1 - r/a)$. Thus, the perturbation expansion concerns the inverse scattering length. As clearly evident from Eq. (12), the change of the scattering length depends on the ‘‘starting value’’ a_1 to which the effect is added. In our calculations, CIB effects are generated step by step, which implies that the starting value a_1 is different for each CIB effect. This distorts the relative size of different CIB contributions to the scattering length difference. To make the relative comparison meaningful, we have rescaled our results for Δa_{CIB} according to a prescription given by Ericson and Miller [5], which goes as follows. Assume the ‘‘starting value’’ for the scattering length is a_1 and a certain CIB effect brings it up to a_2 . Then, the resulting scattering length difference ($a_1 - a_2$) is rescaled by

$$\Delta a = (a_1 - a_2) \frac{\bar{a} a_{np}}{a_1 a_2} \quad (13)$$

with $\bar{a} = -18.05$ fm and $a_{np} = -23.75$ fm. This will make Δa independent of the choice for a_1 . The numbers given in Table III and IV for Δa_{CIB} are all rescaled according to Eq. (13).

We obtain a total Δa_{CIB} of 4.65 fm which is about 80% of the empirical value of 5.7 fm [Eq. (4)]. For Δr_{CIB} we find a total of 0.115 fm from all effects, consistent with the empirical value [Eq. (5)]. Even though our total result for Δa_{CIB} is very similar to the earlier calculation of Ref. [3], there are some differences in the details. For the total effect from 2π -exchange we obtain in the present calculations $\Delta a_{CIB} = 0.36$ fm while in Ref. [3] 0.85 fm was reported. This is due to differences in the interpretation of the scaling mass that occurs in the $N\Delta\pi$ Lagrangian, Eq. (8). While in the present calculations we always use m_{π^\pm} [see discussion below Eq. (8)], in the earlier calculations of Ref. [3] m_{π^0} was used for π^0 coupling and m_{π^\pm} for π^\pm coupling. The latter convention introduces a strong charge-dependence of the effective $N\Delta\pi$ coupling strength, which enhances the CIB effects from all diagrams involving Δ -isobars. In principle, there is discretion in how to deal with the scaling mass in Eq. (8). However, in the present calculations, we decided to follow the established convention [12]. As a result, the effect from 2π -exchange is smaller than in the earlier calculation of Ref. [3].

There is also a small difference in the Δa_{CIB} contribution from non-iterative $\pi\sigma$ and $\pi\omega$ exchanges for which we obtain 1.4 fm while Ref [3] reported 1.2 fm. This discrepancy is due to the fact that in Ref. [3] a preliminary version of the Bonn Full Model [4] was used, while here

we applied the final version [8] in which the strength of the $\pi\sigma$ contribution is slightly larger, which explains the difference.

We note that the CIB effect depends on the πNN coupling constant. In the present calculations, we follow the Bonn model [8]: we assume charge-independence of the coupling constant and use $g_\pi^2/4\pi = 14.4$ [13]. In recent years, there has been some controversy about the precise value of the πNN coupling constant. Unfortunately, the problem is far from being settled. Based upon NN phase shift analysis, the Nijmegen group [14] advocates the ‘‘small’’ charge-independent value $g_\pi^2/4\pi = 13.5(1)$, while a very recent determination by the Uppsala group [15] based upon high precision np charge-exchange data at 162 MeV resulted in the ‘‘large’’ value $g_{\pi^\pm}^2/4\pi = 14.52(26)$. Other recent determinations are in-between the two extremes: The VPI group [16] quotes $g_\pi^2/4\pi = 13.77(15)$ from πN and NN analysis with no evidence for charge-dependence. Bugg and Machleidt [17] obtain $g_{\pi^\pm}^2/4\pi = 13.69(39)$ and $g_{\pi^0}^2/4\pi = 13.94(24)$ from the analysis of NN elastic data between 210 and 800 MeV. Because of this large uncertainty in the πNN coupling constant, it might be of interest to know what the CIB effects are like when a value is used that deviates substantially from our choice. For that reason, we have repeated our CIB calculations with the smaller values $g_\pi^2/4\pi = 14.0$ and 13.6. It turns out that the total CIB effect on phase shifts (last column of Table I) as well as the effect on the effective range parameters (Table III) scales linearly with the πNN coupling constant, to a good approximation. To be precise: multiplying the total phase shift differences in Table I or the effective range changes in Table III with 13.6/14.4 reproduces within $\pm 2\%$ the exact results from a CIB calculation that employs $g_\pi^2/4\pi = 13.6$.

As last item in our study, we have also investigated the effect of rho-mass splitting on the 1S_0 effective range parameters. Unfortunately, the evidence for rho-mass splitting is very uncertain, with the Particle Data Group [11] reporting $m_{\rho^0} - m_{\rho^\pm} = 0.3 \pm 2.2$ MeV. Consistent with this, we assumed in our exploratory study $m_{\rho^0} = 769$ MeV and $m_{\rho^\pm} = 768$ MeV, i. e., a splitting of 1 MeV. With this, we find $\Delta a_{CIB} = -0.29$ fm from one-rho-exchange, and $\Delta a_{CIB} = 0.28$ fm from the non-iterative $\pi\rho$ diagrams with NN intermediate states. Thus, individual effects are small and, in addition, there are substantial cancellations between the two classes of diagrams that contribute. The net result is a vanishing effect. Thus, even if the rho-mass splitting will be better determined in the future and may turn out to be larger than our assumption, it will never be a great source of CIB.

III. SUMMARY AND CONCLUSIONS

Based upon the Bonn meson-exchange model for the NN interaction, we have calculated the CIB effects due to pion-mass splitting on the singlet effective range parameters and on the phase shifts of NN scattering for partial waves of total angular momentum $J \leq 4$ and laboratory energies below 300 MeV. This investigation complements our recent paper on charge-asymmetry of the NN interaction [7].

The overall results may be characterized as follows.

The largest phase shift differences occur in the 1S_0 state where they are most noticeable at low energy; e. g., at 1 MeV, the difference is 4.36^0 , indicating that the np nuclear force is more attractive than the pp nuclear force. The 1S_0 phase shift difference decreases with increasing energy and is about 0.6^0 at 300 MeV. The major part of the phase shift difference comes from OPE. CIB contributions from two-meson exchange diagrams can be large, but there are typically cancellations between the effects from different classes of diagrams of the two-meson type.

The CIB effect on the phase shifts of P and higher partial waves is generally small. The most significant difference is found in the 3P_0 state around 50 MeV where the difference is almost 1 degree. In P -waves, the difference is roughly constant above 25 MeV: it is $0.95\text{--}0.65^0$ in 3P_0 , about 0.35^0 in 3P_1 , and around 0.2^0 in 3P_2 . In all other partial waves, it is in the order of 0.1^0 or less. Again, the main effect comes from OPE, however, in 3P_0 , 3P_1 , and 1D_2 at 300 MeV, the effect from the 2π model is in the range of 20 - 50% of the one from OPE.

The fact that the magnitudes of the phase shift differences in all partial waves, except 1S_0 , are small, makes it difficult to verify experimentally the charge dependent effects in P and higher partial waves. However, since the phase shifts in these states themselves are small, the relative magnitudes of the phase shift differences are not negligible and could have a noticeable effect on some sensitive observables such as the analyzing power (A_y) in nucleon-deuteron (nd) scattering [18] since this reaction blows up effects from triplet P waves [19]. Our microscopic predictions are, however, substantially smaller than what is needed to solve the nd A_y puzzle [18,20].

As mentioned in the Introduction, another CIB contribution to the nuclear force is irreducible pion-photon ($\pi\gamma$) exchange. Traditionally, it was believed that this contribution would take care of the remaining 20% of Δa_{CIB} [5,2]. However, a recently derived $\pi\gamma$ potential based upon chiral perturbation theory [21] decreases Δa_{CIB} by about 0.6 fm, making the discrepancy even larger. Thus, we are faced with the fact that about 20 - 30% of the charge-dependence of the singlet scattering length is not explained.

In recent years, nuclear physicists have become increasingly concerned with chiral symmetry which is an approximate symmetry of QCD in the light-quark sector. In the light of these new views, the NN interaction

should have a clear relationship with chiral symmetry. The Bonn model that our investigation is based upon is, by construction, not a consistently chiral model. Chiral models for the NN interaction and, in particular, chiral models for the 2π exchange have recently been constructed by various groups [22–24]. However, most of these models are applicable only for the peripheral partial waves of NN scattering and not for S , P , or D waves; and if there are predictions for lower partial waves, they are only of qualitative nature. The CIB effects in S and P waves and, particularly, for the singlet scattering length are very subtle and, therefore, require a quantitative model. Thus, current chiral models for the 2π exchange are not (yet) suitable for reliable calculations of CIB. One may then raise an interesting question: What has to be changed in the Bonn model to make it chiral? This question can be answered precisely. The diagrams in Figs. 2 (a) and (b) of Ref. [22] have to be added to the Bonn model; that is essentially all. These diagrams include the Weinberg-Tomozawa $\pi\pi NN$ vertex which is a characteristic ingredient of any nonlinear realization of chiral symmetry. However, it has been found independently by different groups [22–24] that the 2π exchange diagrams which include the Weinberg-Tomozawa vertex make a very small, essentially negligible, contribution to the NN interaction. One may then expect that the CIB caused by these diagrams is also very small [25]. Thus, there are reasons to believe that the results of this study may be of broader relevance than what the (formally) non-chiral character of our model suggests. Of course, the final and reliable answer of the question under consideration can only come from a ‘perfect’ and quantitative chiral model for the NN interaction that is applicable also in S waves and for the calculation of scattering lengths. In view of the problems raised concerning scattering length calculations with chiral models [26,27] and in view of the continuing general controversy concerning cutoff *versus* dimensional regularization, it will take many years until a reliable calculation of this kind can be done. Thus, for the time being, it may be comforting to have at least our present results.

This work was supported in part by the U.S. National Science Foundation under Grant No. PHY-9603097 and by the Idaho State Board of Education.

[1] G. A. Miller, B. M. K. Nefkens, and I. Slaus, Phys. Reports **194**, 1 (1990).

[2] G. A. Miller and W. H. T. van Oers, In *Symmetries and Fundamental Interactions in Nuclei*, W. C. Haxton and E. M. Henley, eds. (World Scientific, Singapore, 1995) p. 127.

[3] C. Y. Cheung and R. Machleidt, Phys. Rev. C **34** 1181 (1986).

[4] R. Machleidt, in *Quarks and Nuclear Structure*, Proc. 3rd Klaus Erkelenz Symposium, Bad Honnef, 1983, Lecture Notes in Physics, Vol. 197, edited by K. Bleuler (Springer, Heidelberg, 1984), p. 352

[5] T. E. O. Ericson and G. A. Miller, Phys. Lett. **132B**, 32 (1983).

[6] M. H. Partovi and E. L. Lomon, Phys. Rev. D **2**, 1999 (1970).

[7] G. Q. Li and R. Machleidt, *Charge-Asymmetry of the Nucleon-Nucleon Interaction*, nucl-th/9804023; Phys. Rev. C, in press.

[8] R. Machleidt, K. Holinde, and Ch. Elster, Phys. Reports **149**, 1 (1987).

[9] R. Machleidt, Adv. Nucl. Phys. **19**, 189 (1989).

[10] R. Machleidt and G. Q. Li, Phys. Reports **242**, 5 (1994).

[11] Particle Data Group, Review of Particle Properties, Phys. Rev. D **45** (1992).

[12] O. Dumbrajs *et al.*, Nucl. Phys. **B216**, 277 (1983).

[13] The relationship between g_π and $f_{\pi NN}$ [the latter being used in the Lagrangian Eq. (7)] is

$$g_\pi^2 = \left(\frac{2M_N}{m_{\pi^\pm}} \right)^2 f_{\pi NN}^2 = 181.027 f_{\pi NN}^2 .$$

Following the Bonn model [8], we also assume a fixed relationship between $f_{\pi N\Delta}$ [used in the Lagrangian Eq. (8)] and $f_{\pi NN}$, namely,

$$f_{\pi N\Delta}^2 = \frac{72}{25} f_{\pi NN}^2 .$$

[14] V. Stoks, R. Timmermans, and J. J. de Swart, Phys. Rev. C **47**, 512 (1993).

[15] J. Rahm *et al.*, Phys. Rev. C **57**, 1077 (1998).

[16] R. A. Arndt, R. L. Workman, and M. M. Pavan, Phys. Rev. C **49**, 2729 (1994); R. A. Arndt, I. I. Strakovsky, and R. L. Workman, *ibid.*, **52**, 2246 (1995).

[17] D. V. Bugg and R. Machleidt, Phys. Rev. C **52**, 1203 (1995).

[18] H. Witala and W. Glöckle, Nucl. Phys. **A528**, 48 (1991); W. Glöckle, H. Witala, D. Hüber, H. Kamada, and J. Golak, Phys. Reports **274**, 107 (1996).

[19] I. Slaus, R. Machleidt, W. Tornow, W. Glöckle, and W. Witala, Comments Nucl. Part. Phys. **20**, 85 (1991).

[20] D. Hueber and J. L. Friar, *The A_y Puzzle and the Nuclear Force*, nucl-th/9803038.

[21] U. van Kolck, M. C. M. Rentmeester, J. L. Friar, T. Goldman, and J. J. de Swart, Phys. Rev. Lett. **80**, 4386 (1998).

[22] C. Ordonez, L. Ray, and U. van Kolck, Phys. Rev. C **53**, 2086 (1996).

[23] M. R. Robilotta and C. A. da Rocha, Nucl. Phys. **A615**, 391 (1997).

[24] N. Kaiser, R. Brockmann, and W. Weise, Nucl. Phys. **A625**, 758 (1997).

[25] U. van Kolck, privat communication.

[26] K. A. Scaldeferri, D. R. Philipps, C. W. Kao, and T. D. Cohen, Phys. Rev. C **56**, 679 (1997).

[27] D. B. Kaplan, M. B. Savage, and M. B. Wise, Nucl. Phys. **B478**, 629 (1996).

TABLE I. CIB phase differences (in degrees) as defined in Eqs. (9) and (10) and explained in the text.

T_{lab} (MeV)	OPE	2π	$\pi\rho$	$\pi\sigma + \pi\omega$	Total
1S_0					
1	3.051	0.319	-0.361	1.355	4.364
5	1.767	0.154	-0.193	0.719	2.446
10	1.364	0.103	-0.147	0.545	1.864
25	0.944	0.047	-0.107	0.391	1.275
50	0.712	0.009	-0.090	0.318	0.950
100	0.563	-0.031	-0.083	0.276	0.725
150	0.519	-0.061	-0.086	0.267	0.638
200	0.509	-0.091	-0.093	0.269	0.595
300	0.544	-0.163	-0.121	0.300	0.559
3P_0					
1	-0.032	0.000	0.000	0.000	-0.032
5	-0.246	-0.003	0.000	-0.001	-0.250
10	-0.482	-0.009	0.001	-0.002	-0.492
25	-0.827	-0.029	0.002	-0.005	-0.858
50	-0.902	-0.053	0.005	-0.009	-0.960
100	-0.786	-0.078	0.008	-0.012	-0.869
150	-0.685	-0.091	0.009	-0.011	-0.778
200	-0.618	-0.101	0.011	-0.009	-0.717
300	-0.540	-0.118	0.012	-0.002	-0.648
3P_1					
1	0.017	0.000	0.000	0.000	0.017
5	0.116	0.001	0.000	0.000	0.117
10	0.203	0.002	0.000	0.001	0.206
25	0.313	0.007	-0.001	0.003	0.322
50	0.346	0.016	-0.004	0.008	0.366
100	0.323	0.032	-0.009	0.018	0.364
150	0.289	0.046	-0.014	0.028	0.349
200	0.259	0.058	-0.020	0.037	0.335
300	0.213	0.083	-0.032	0.057	0.321
1D_2					
5	-0.009	0.000	0.000	0.000	-0.009
10	-0.025	0.000	0.000	0.000	-0.025
25	-0.052	0.001	0.000	0.000	-0.050
50	-0.045	0.005	0.000	0.000	-0.040
100	0.003	0.015	-0.001	0.001	0.018
150	0.044	0.025	-0.001	0.001	0.069
200	0.071	0.034	-0.002	0.002	0.106
300	0.100	0.047	-0.002	0.002	0.147
3P_2					
5	-0.010	0.000	0.000	0.000	-0.011
10	-0.030	0.000	0.000	-0.001	-0.032
25	-0.096	-0.001	-0.001	-0.003	-0.101
50	-0.172	-0.003	-0.002	-0.007	-0.184
100	-0.224	-0.007	-0.005	-0.014	-0.250
150	-0.224	-0.007	-0.007	-0.019	-0.258
200	-0.210	-0.007	-0.008	-0.022	-0.248
300	-0.183	-0.004	-0.010	-0.022	-0.219
3F_2					
10	-0.004	0.000	0.000	0.000	-0.004
25	-0.020	0.000	0.000	0.000	-0.020

50	-0.045	0.000	0.000	0.000	-0.045
100	-0.070	-0.001	0.000	0.000	-0.071
150	-0.084	-0.001	0.000	0.000	-0.084
200	-0.093	-0.001	0.000	0.000	-0.093
300	-0.102	-0.001	-0.001	0.001	-0.102
ϵ_2					
5	0.012	0.000	0.000	0.000	0.012
10	0.036	0.000	0.000	0.000	0.036
25	0.091	0.001	0.000	0.000	0.092
50	0.119	0.002	0.000	0.001	0.121
100	0.095	0.007	-0.001	0.001	0.102
150	0.057	0.011	-0.002	0.002	0.068
200	0.025	0.014	-0.003	0.003	0.038
300	-0.018	0.018	-0.006	0.003	-0.003
3F_3					
10	0.009	0.000	0.000	0.000	0.009
25	0.044	0.000	0.000	0.000	0.044
50	0.093	0.000	0.000	0.000	0.093
100	0.141	0.001	0.000	0.000	0.142
150	0.159	0.003	0.000	0.000	0.163
200	0.166	0.005	0.000	0.001	0.171
300	0.165	0.010	-0.001	0.002	0.177
1G_4					
25	-0.009	0.000	0.000	0.000	-0.009
50	-0.023	0.000	0.000	0.000	-0.023
100	-0.032	0.001	0.000	0.000	-0.032
150	-0.029	0.002	0.000	0.000	-0.027
200	-0.022	0.003	0.000	0.000	-0.019
300	-0.005	0.006	0.000	0.000	0.001
3F_4					
25	-0.004	0.000	0.000	0.000	-0.004
50	-0.015	0.000	0.000	0.000	-0.015
100	-0.037	0.000	0.000	0.000	-0.037
150	-0.053	0.000	0.000	0.000	-0.053
200	-0.064	0.000	0.000	-0.001	-0.065
300	-0.078	-0.001	0.000	-0.001	-0.080
3H_4					
50	-0.007	0.000	0.000	0.000	-0.007
100	-0.019	0.000	0.000	0.000	-0.019
150	-0.028	0.000	0.000	0.000	-0.029
200	-0.035	0.000	0.000	0.000	-0.036
300	-0.044	-0.001	0.000	0.000	-0.045
ϵ_4					
25	0.012	0.000	0.000	0.000	0.012
50	0.033	0.000	0.000	0.000	0.033
100	0.058	0.000	0.000	0.000	0.059
150	0.067	0.001	0.000	0.000	0.068
200	0.068	0.001	0.000	0.000	0.070
300	0.062	0.002	0.000	0.000	0.065

TABLE II. CIB phase shift differences (in degrees) as defined in Eq. (9) for the various 2π -exchange contributions explained in the text. S denotes stretched-box diagrams, B box, and X crossed-box diagrams.

T_{lab} (MeV)	$2\pi NN-S$	$2\pi NN-X$	$2\pi N\Delta-B$	$2\pi N\Delta-X$	$2\pi\Delta\Delta-B$	$2\pi\Delta\Delta-X$	Total 2π
1S_0							
1	-0.182	0.319	0.692	-0.410	-0.244	0.143	0.319
5	-0.098	0.160	0.363	-0.217	-0.130	0.076	0.154
10	-0.075	0.113	0.271	-0.165	-0.099	0.058	0.103
25	-0.056	0.065	0.188	-0.119	-0.072	0.042	0.047
50	-0.047	0.037	0.146	-0.099	-0.061	0.034	0.009
100	-0.045	0.012	0.118	-0.091	-0.056	0.030	-0.031
150	-0.047	-0.003	0.109	-0.093	-0.058	0.030	-0.061
200	-0.052	-0.015	0.107	-0.100	-0.062	0.031	-0.091
300	-0.067	-0.041	0.112	-0.126	-0.078	0.037	-0.163
3P_0							
10	-0.003	-0.003	0.001	-0.003	0.000	0.000	-0.009
25	-0.010	-0.010	0.002	-0.009	-0.001	0.000	-0.029
50	-0.018	-0.020	0.002	-0.017	-0.002	0.000	-0.053
100	-0.025	-0.030	0.003	-0.024	-0.002	0.001	-0.078
150	-0.027	-0.036	0.002	-0.028	-0.003	0.001	-0.091
200	-0.029	-0.041	0.002	-0.030	-0.003	0.001	-0.101
300	-0.031	-0.050	0.000	-0.035	-0.004	0.001	-0.118
3P_1							
10	0.000	0.002	0.001	-0.001	0.000	0.000	0.002
25	-0.001	0.006	0.004	-0.002	0.000	0.000	0.007
50	-0.002	0.012	0.010	-0.003	-0.001	0.001	0.016
100	-0.003	0.021	0.021	-0.006	-0.001	0.001	0.032
150	-0.004	0.028	0.030	-0.008	-0.002	0.002	0.046
200	-0.004	0.034	0.038	-0.009	-0.002	0.002	0.058
300	-0.004	0.043	0.054	-0.010	-0.003	0.003	0.083
1D_2							
50	0.000	0.003	0.002	0.000	0.000	0.000	0.005
100	0.000	0.009	0.007	-0.001	0.000	0.000	0.015
150	0.000	0.014	0.013	-0.002	-0.001	0.001	0.025
200	0.000	0.017	0.019	-0.003	-0.001	0.001	0.034
300	0.000	0.020	0.031	-0.004	-0.002	0.002	0.047
3P_2							
10	-0.001	0.001	0.001	-0.001	0.000	0.000	0.000
25	-0.003	0.002	0.005	-0.004	-0.001	0.001	-0.001
50	-0.006	0.004	0.011	-0.010	-0.004	0.002	-0.003
100	-0.009	0.004	0.020	-0.018	-0.008	0.004	-0.007
150	-0.010	0.004	0.027	-0.022	-0.011	0.005	-0.007
200	-0.010	0.003	0.031	-0.024	-0.014	0.007	-0.007
300	-0.009	0.003	0.037	-0.024	-0.018	0.008	-0.004

TABLE III. CIB contributions to the 1S_0 scattering length, Δa_{CIB} , and effective range, Δr_{CIB} , from various components of the NN interaction as explained in the text.

	OPE	2π	$\pi\rho$	$\pi\sigma + \pi\omega$	Total	Empirical
Δa_{CIB} (fm)	3.243	0.360	-0.383	1.426	4.646	5.7 ± 0.5
Δr_{CIB} (fm)	0.099	0.002	-0.006	0.020	0.115	0.05 ± 0.13

TABLE IV. CIB contributions to the 1S_0 scattering length, Δa_{CIB} , and effective range, Δr_{CIB} , for the various parts of the 2π -exchange model as explained in the text. S denotes stretched-box diagrams, B box, and X crossed-box diagrams.

	$2\pi NN-S$	$2\pi NN-X$	$2\pi N\Delta-B$	$2\pi N\Delta-X$	$2\pi\Delta\Delta-B$	$2\pi\Delta\Delta-X$	Total 2π
Δa_{CIB} (fm)	-0.196	0.351	0.787	-0.470	-0.272	0.159	0.360
Δr_{CIB} (fm)	-0.003	0.003	0.010	-0.006	-0.004	0.002	0.002

FIG. 1. One-pion-exchange (OPE) contribution to (a) pp and (b) np scattering.

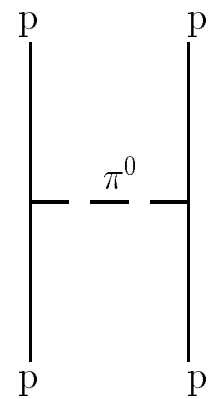
FIG. 2. Irreducible 2π -exchange diagrams with NN intermediate states for (a) pp and (b) np scattering.

FIG. 3. 2π -exchange contributions with $N\Delta$ intermediate states to (a) pp and (b) np scattering.

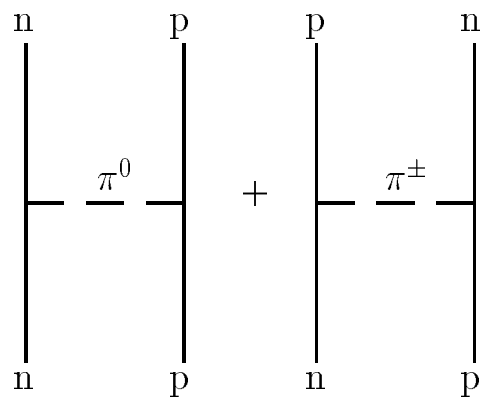
FIG. 4. 2π -exchange contributions with $\Delta\Delta$ intermediate states to (a) pp and (b) np scattering.

FIG. 5. CIB phase shift differences $\Delta\delta_{CIB}^{LSJ}$ (in degrees) as defined in Eq. (9) for laboratory kinetic energies T_{lab} below 300 MeV and partial waves with total angular momentum $J \leq 2$. The CIB effects due to OPE, the entire 2π model, $\pi\rho$ exchanges, and $(\pi\sigma + \pi\omega)$ contributions are shown by the dashed, dash-dot, dash-triple-dot, and dotted curves, respectively. The solid curve is the sum of all CIB effects. (See text for further explanations.)

FIG. 6. Similar to Fig. 5, but here the individual contributions from the 2π model are shown. The CIB effects due to $2\pi NN$, $2\pi N\Delta B$, $2\pi N\Delta X$, and $2\pi\Delta\Delta$ are shown by the dashed, dash-dot, dash-triple-dot, and dotted and $2\pi\Delta\Delta$ are shown by the dashed, dash-dot, dash-triple-dot, and dotted curves, respectively. The solid curve is the sum of all CIB effects due to the exchange of two pions. (See text and caption of Table II for further explanations.)

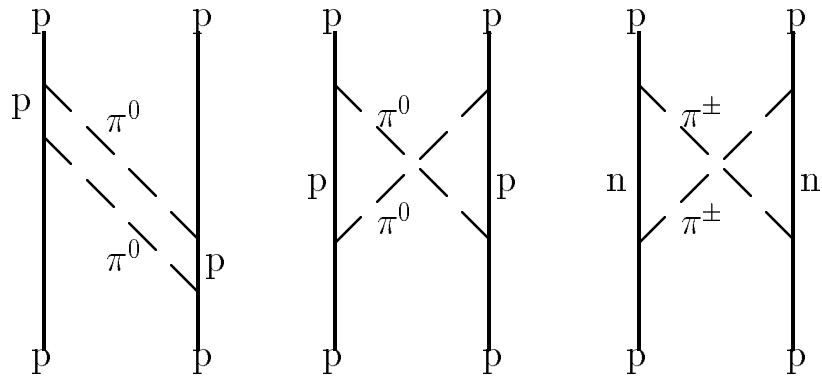


(a)

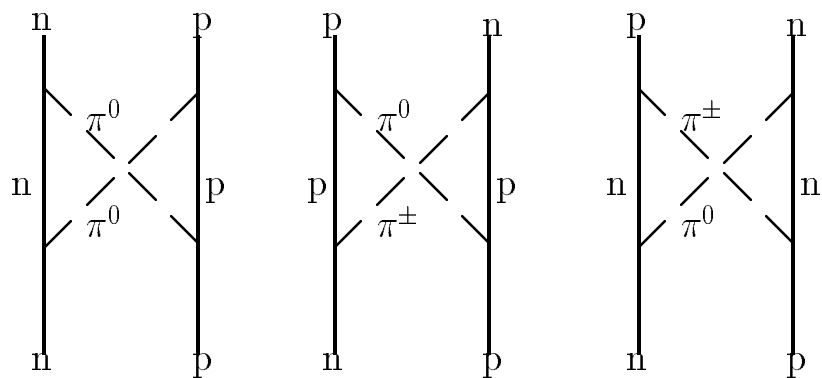
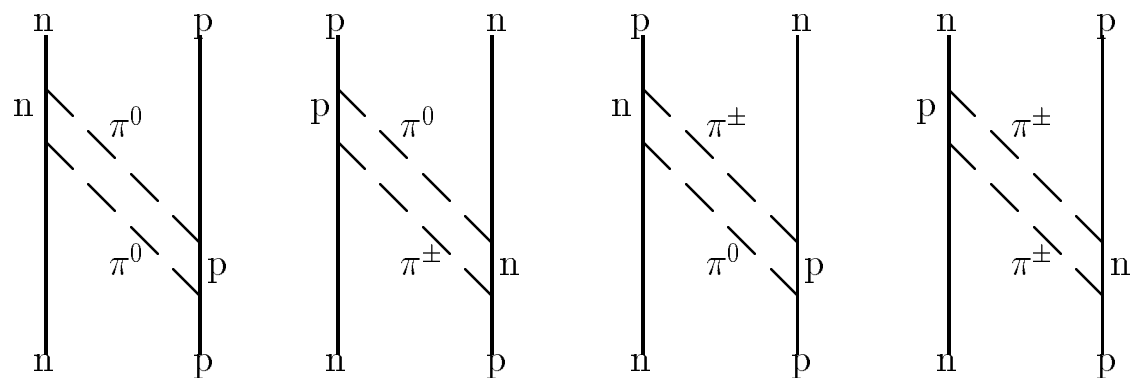


(b)

Li/Machleidt (CIB) Fig. 1

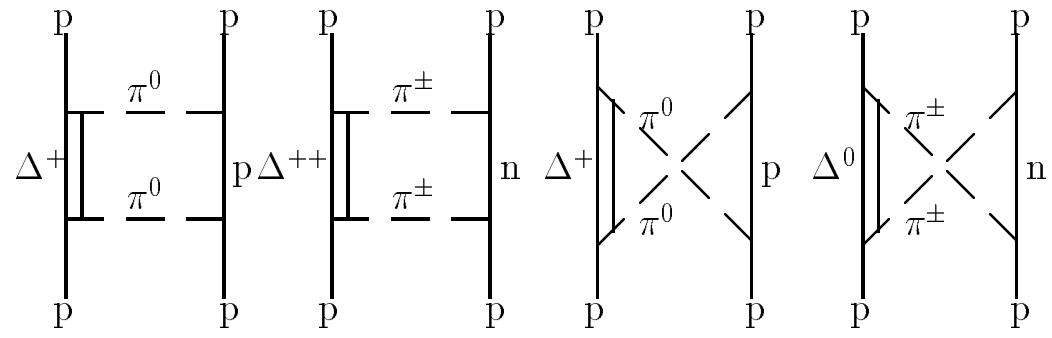


(a)

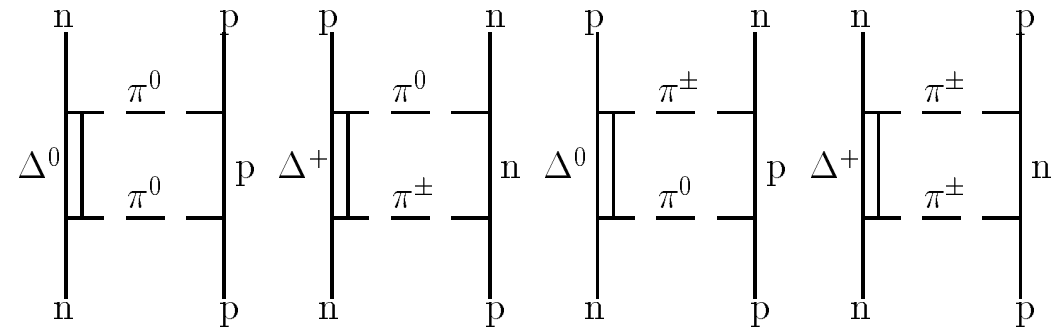


(b)

Li/Machleidt (CIB) Fig. 2

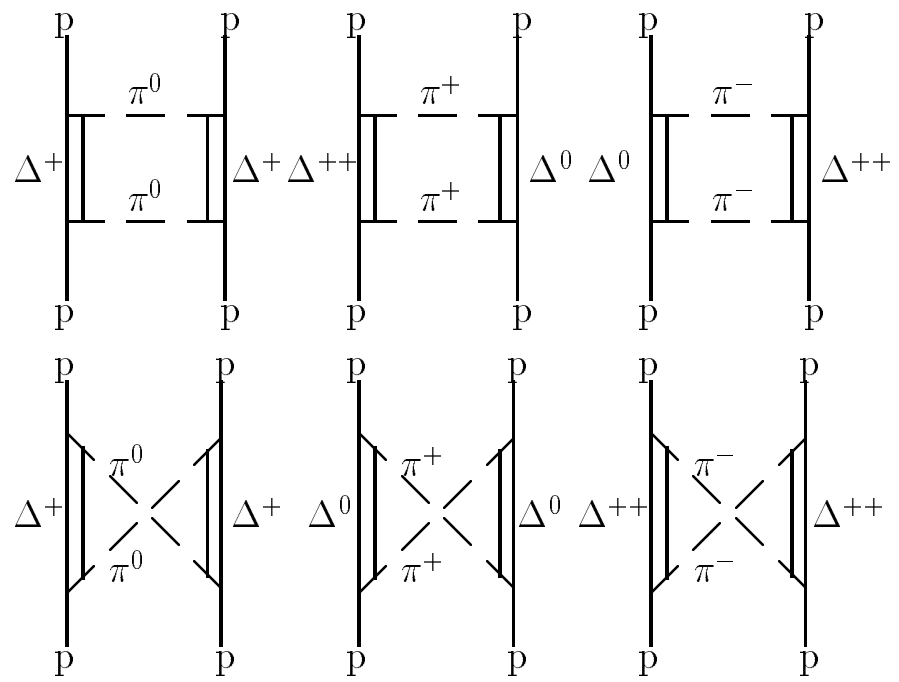


(a)

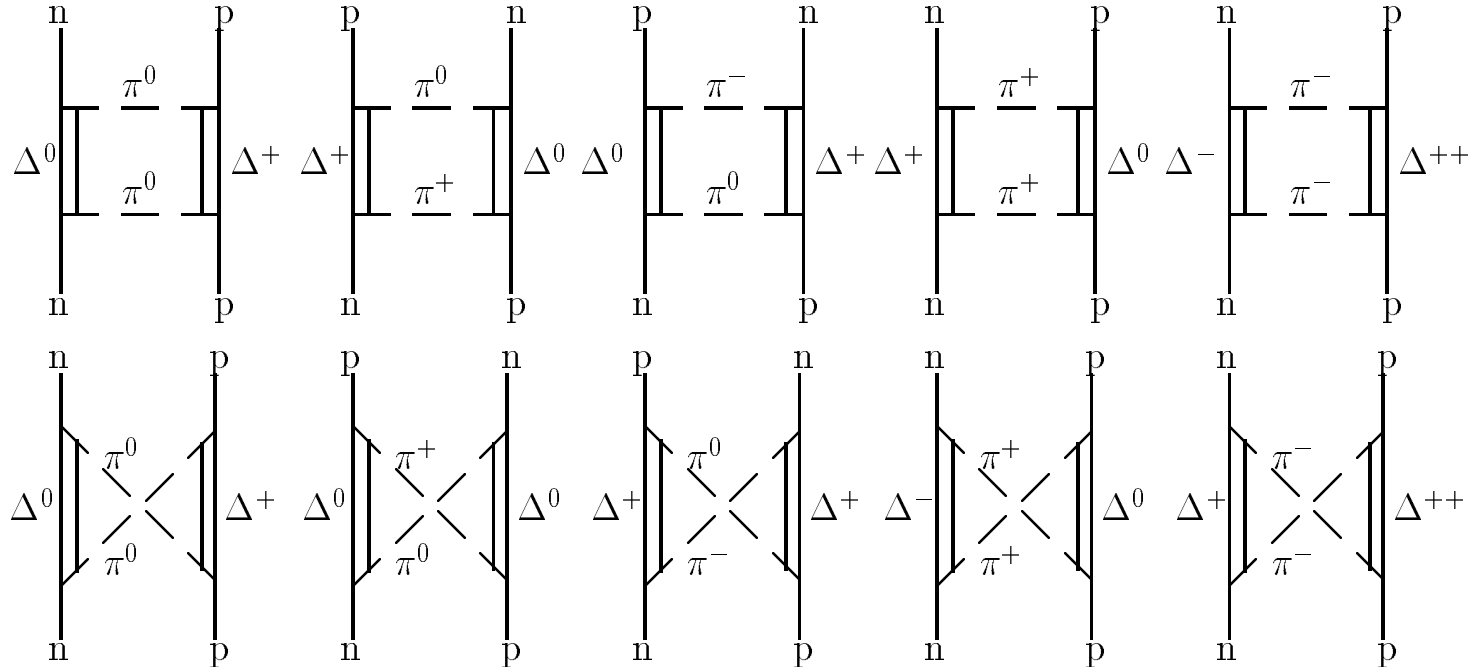


(b)

Li/Machleidt (CIB) Fig. 3

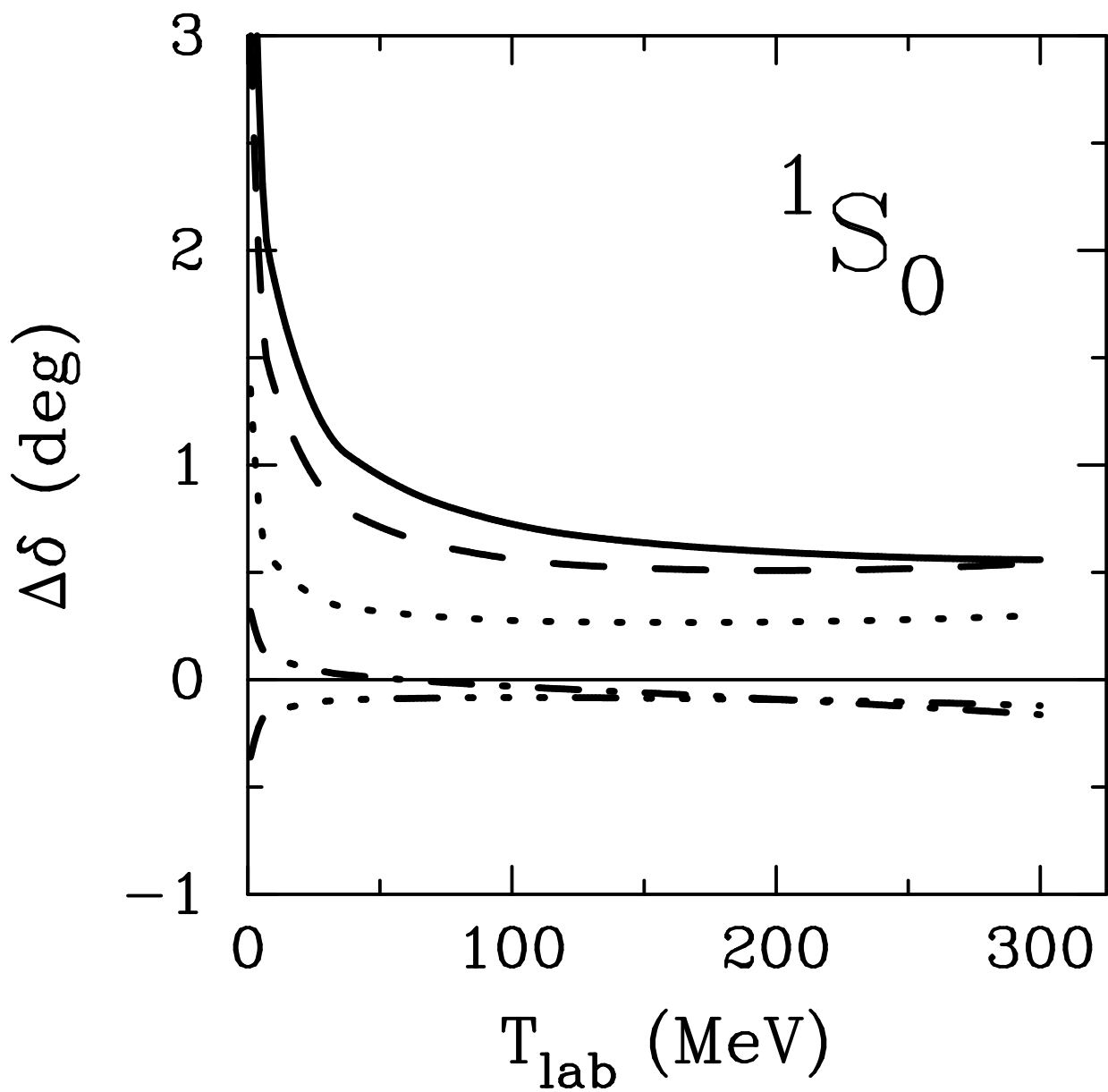


(a)

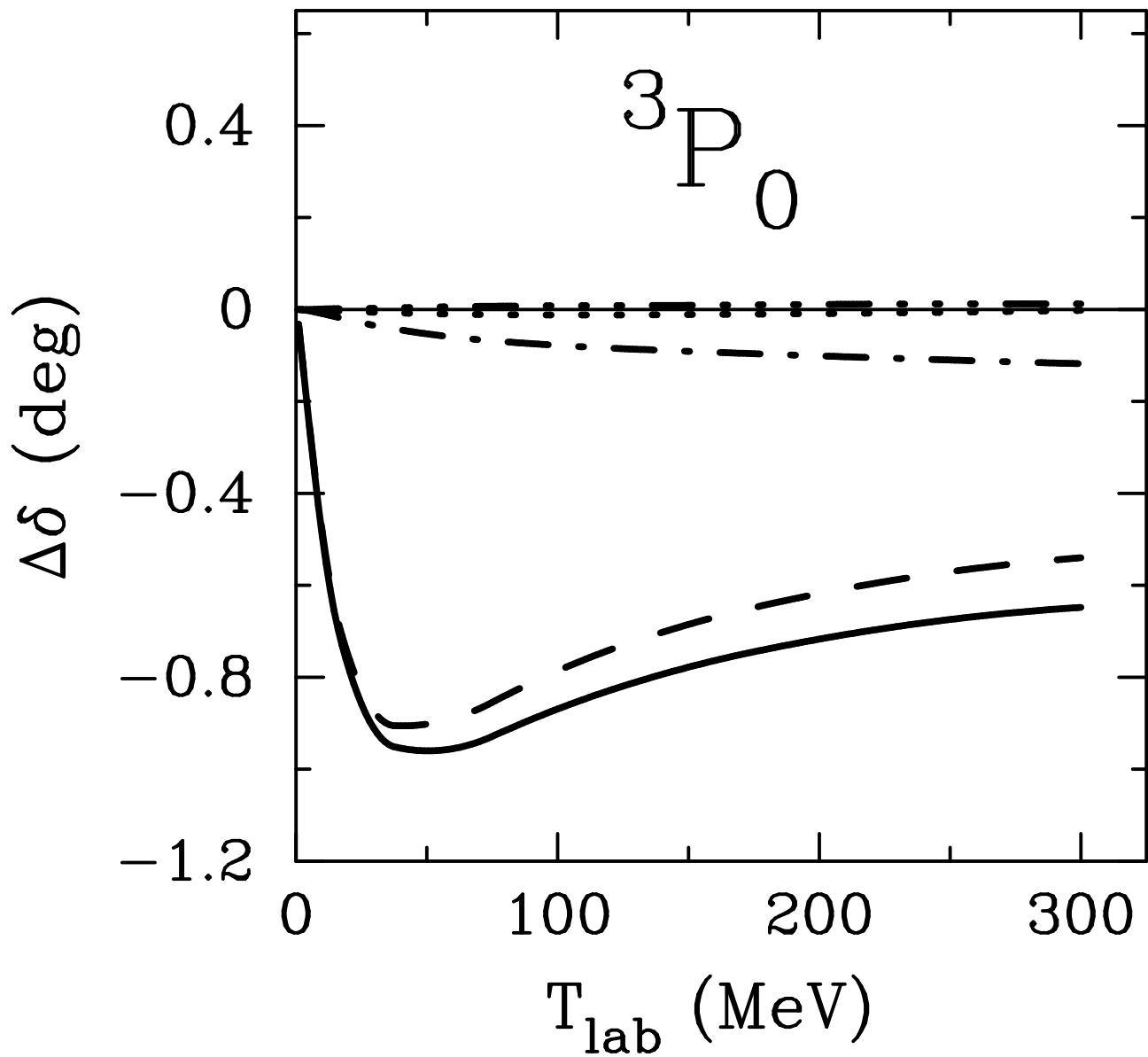


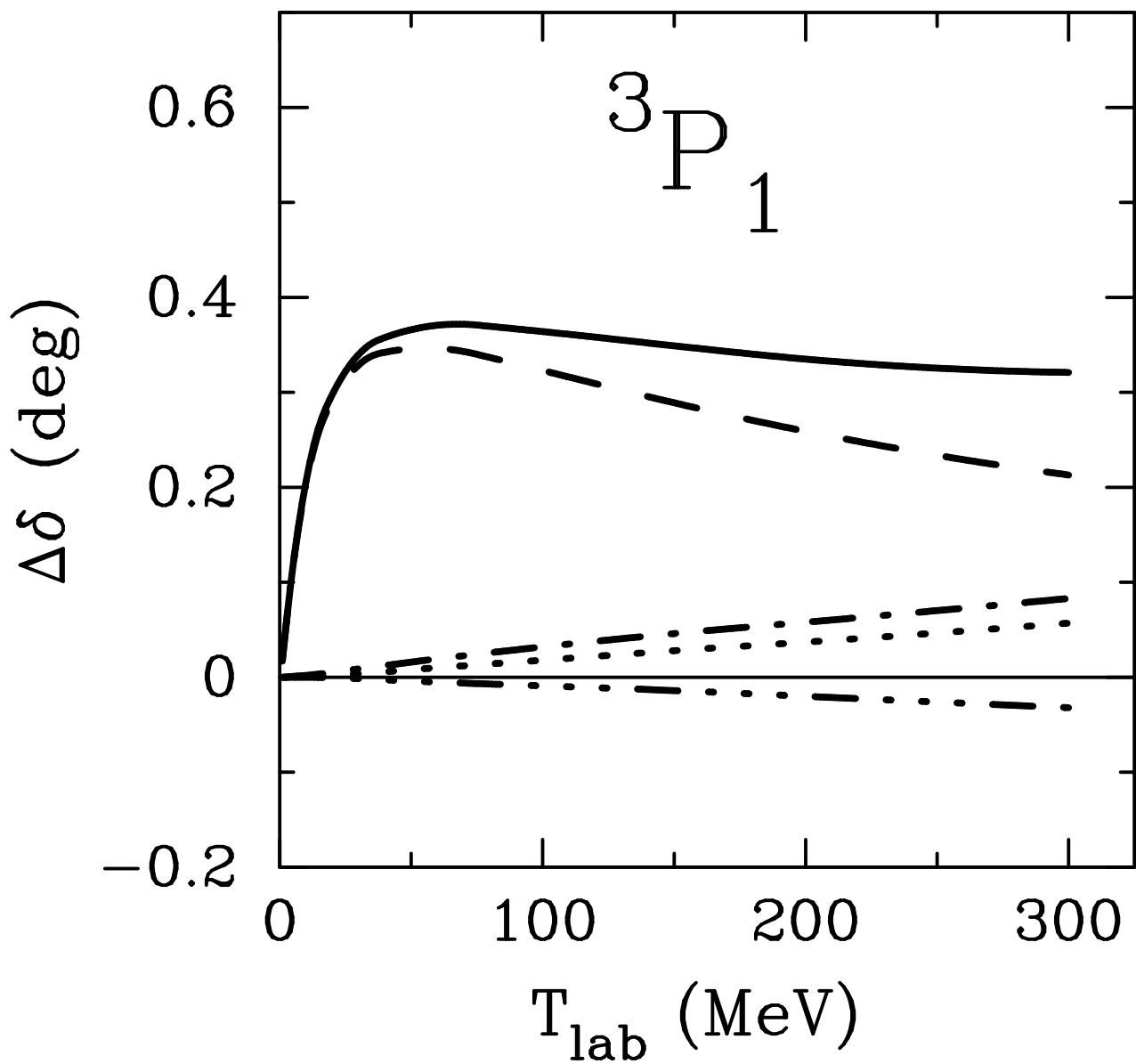
(b)

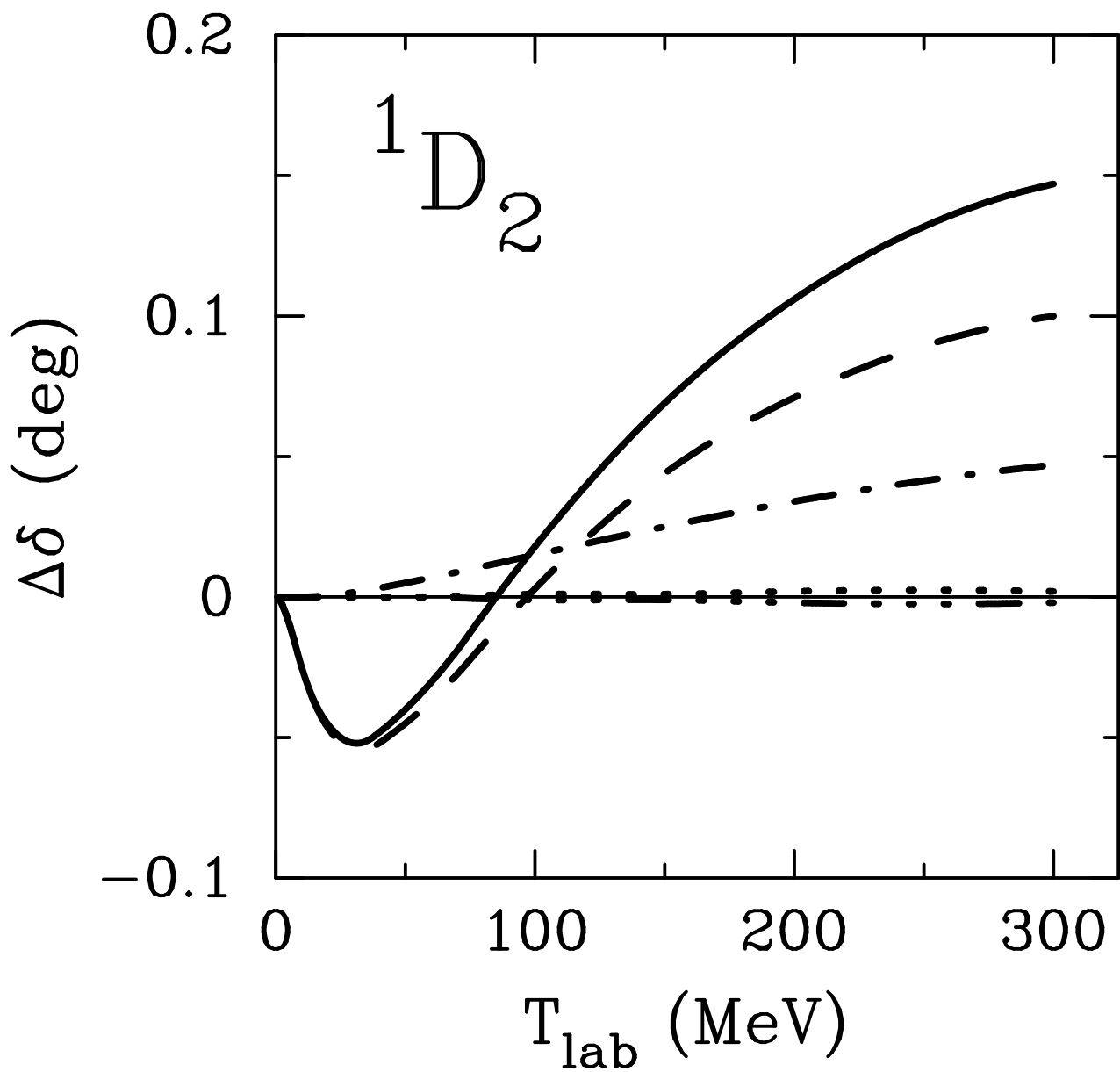
Li/Machleidt (CIB) Fig. 4



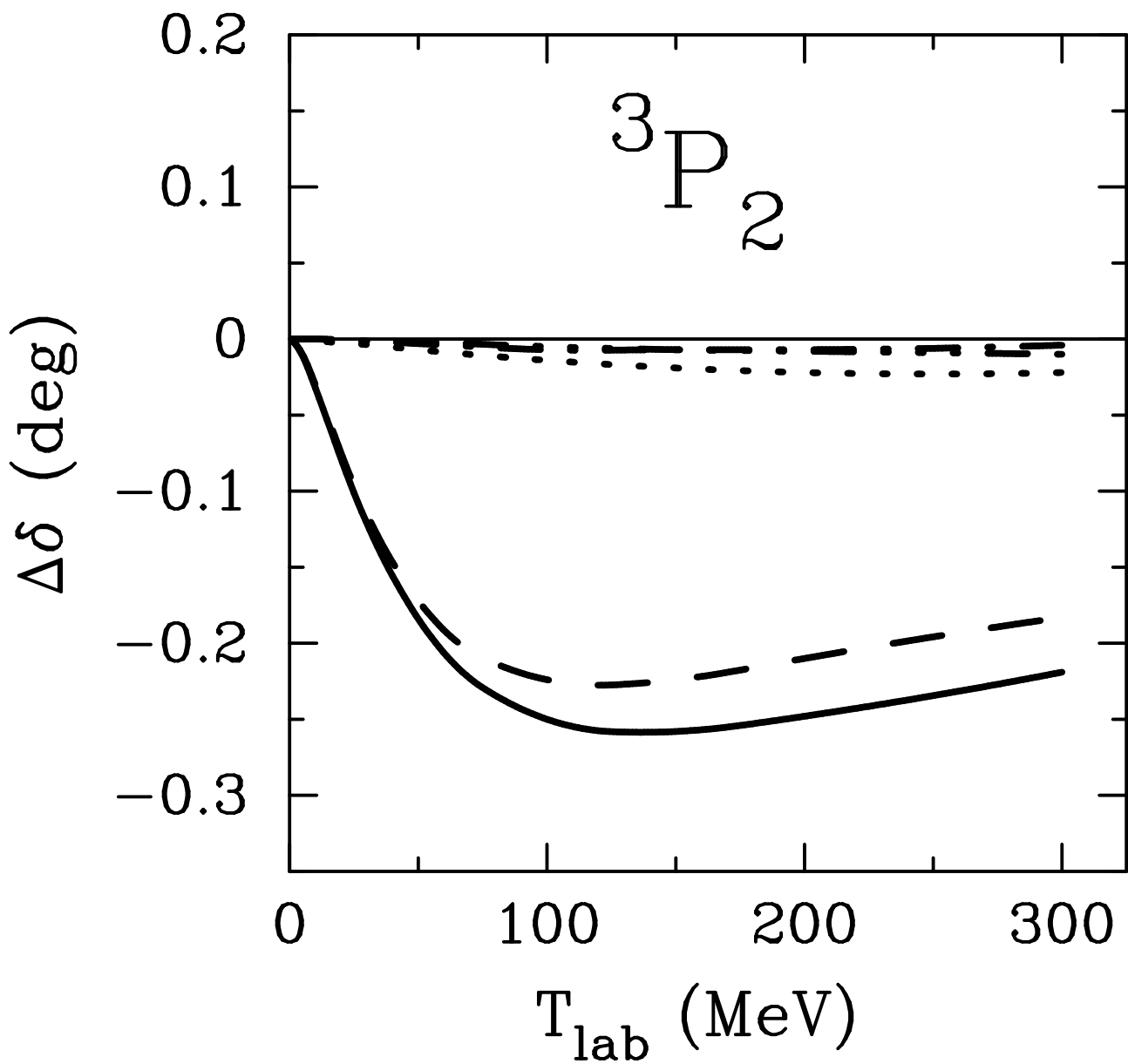
Li/Machleidt (CIB) Fig. 5, part 1 of 5

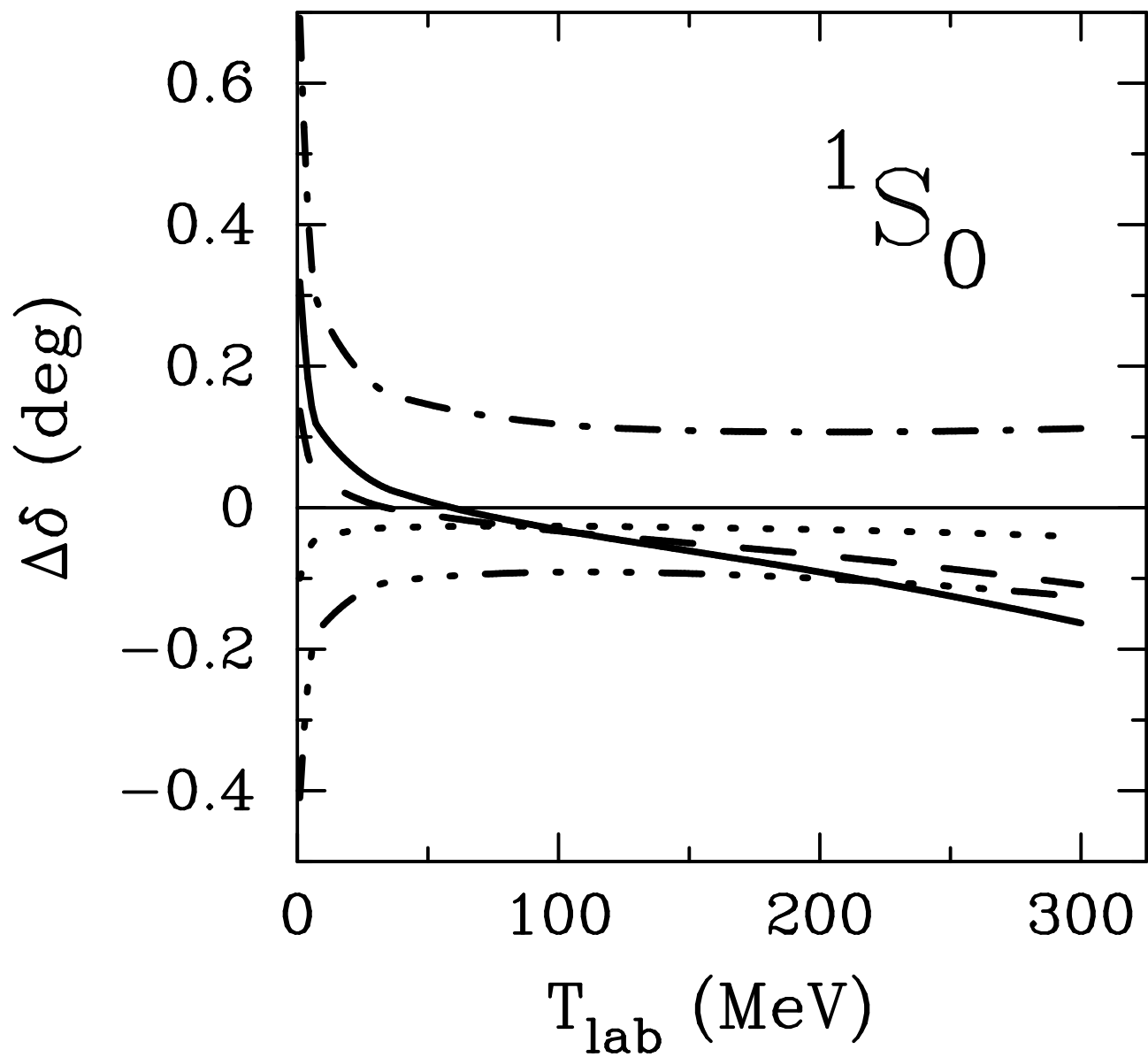


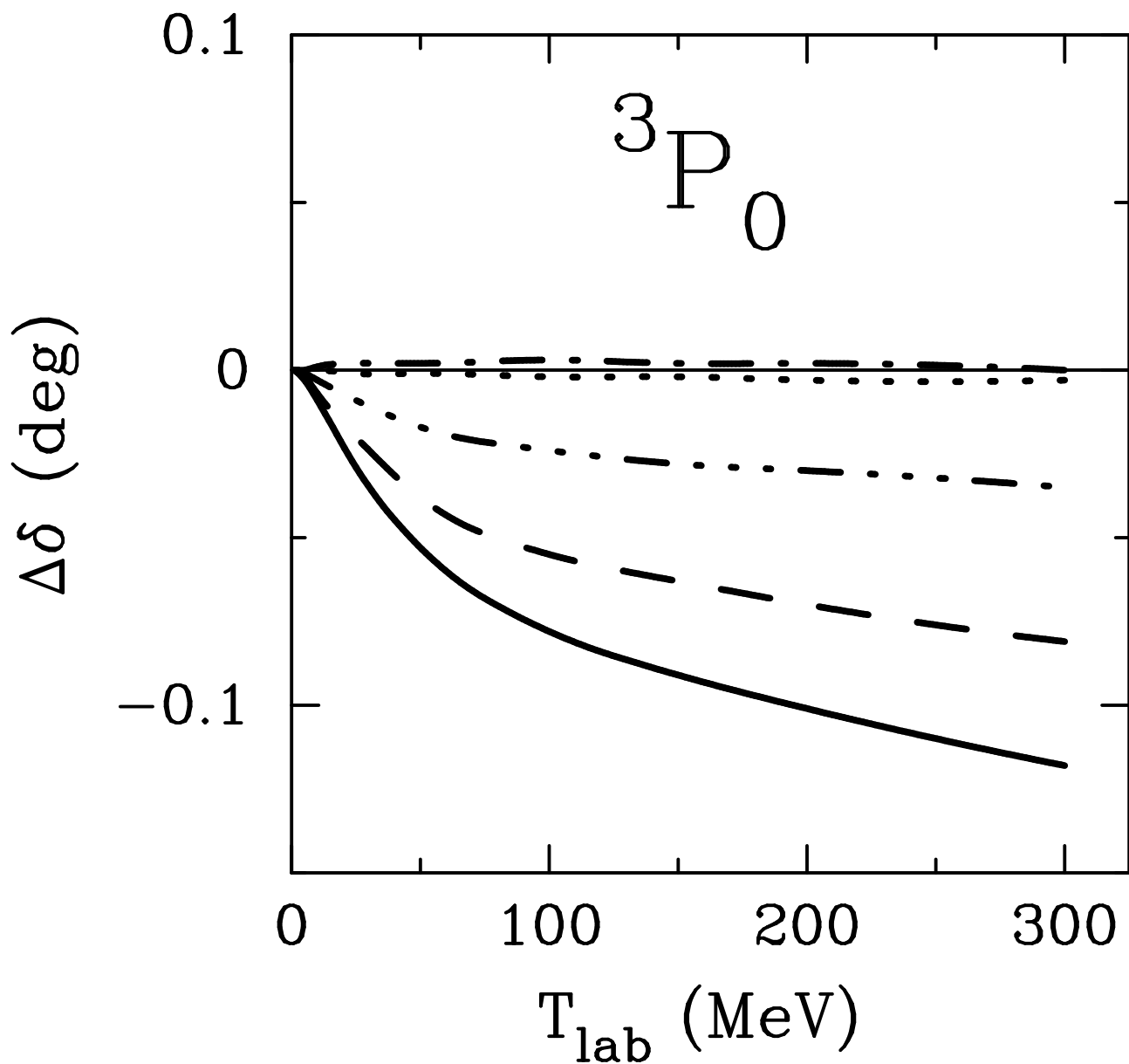


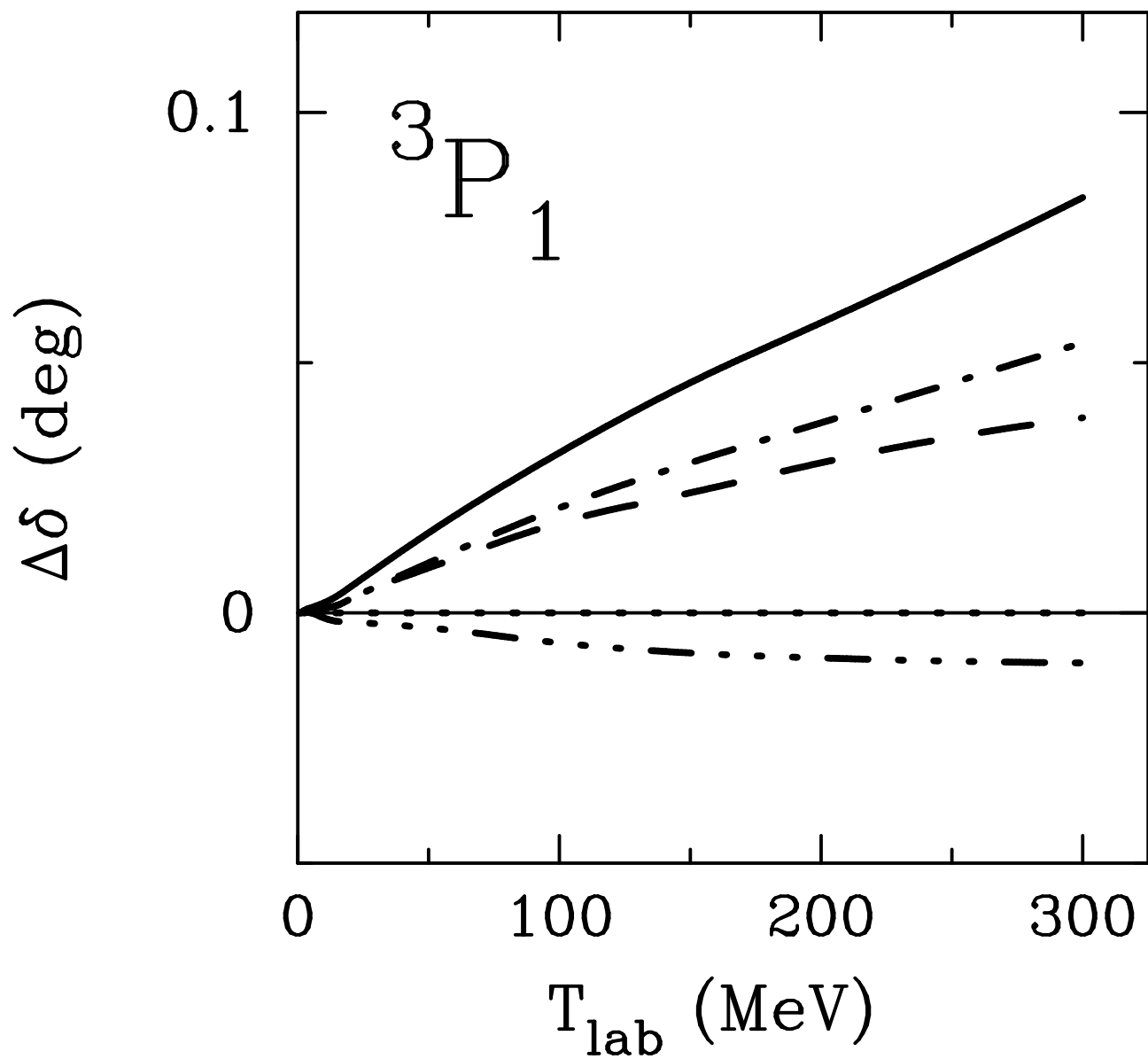


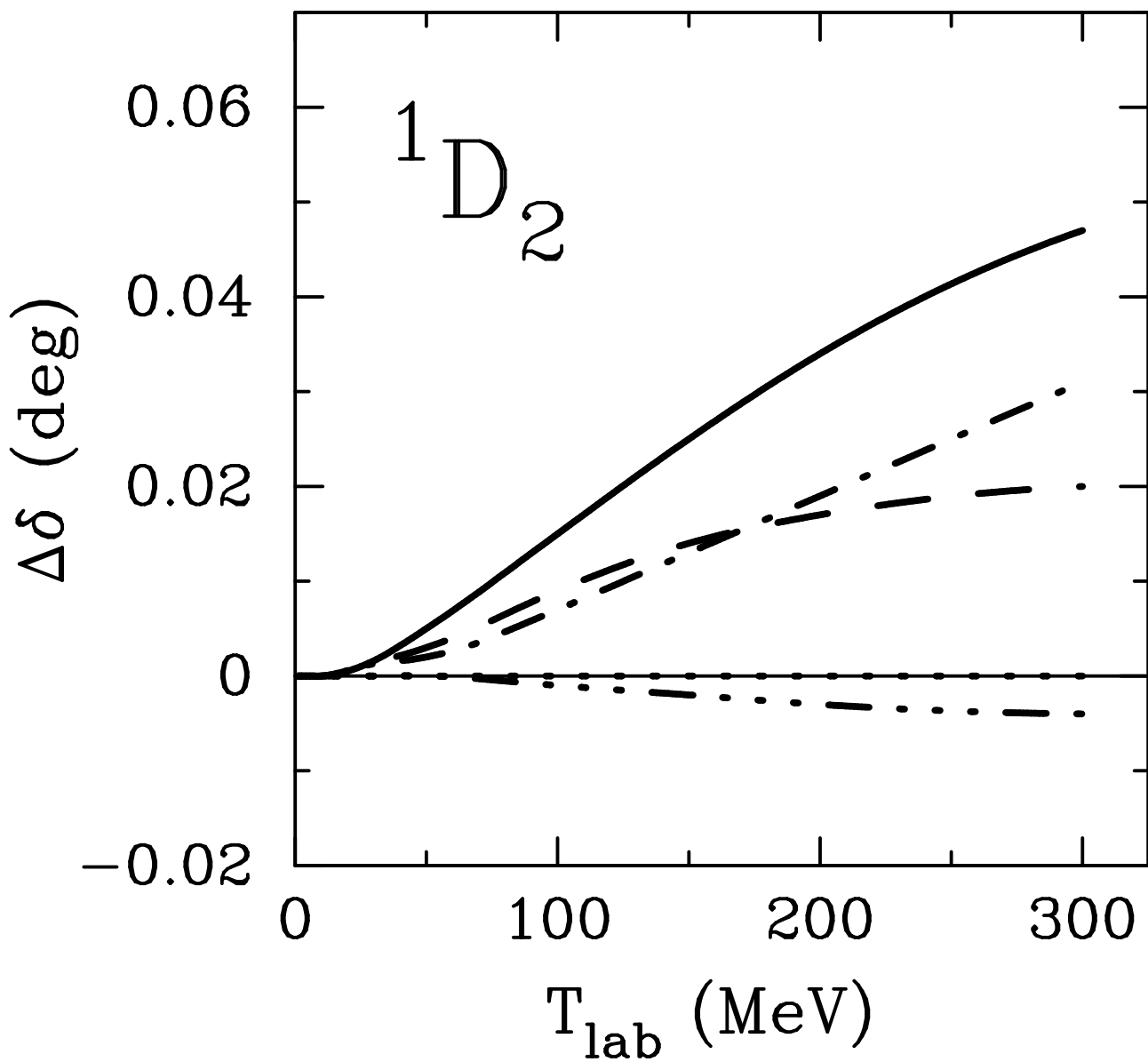
Li/Machleidt (CIB) Fig. 5, part 4 of 5











Li/Machleidt (CIB) Fig. 6, part 4 of 5

